AIRBORNE DIGITAL SENSORS – A NEW APPROACH

P. Fricker[1], R. Sandau[1], A.S. Walker[2]
[1]LH Systems GmbH, Heinrich-Wild-Strasse, CH-9435 Switzerland, fricker/sandau@lh-systems.com
[2]LH Systems, LLC, 10965 Via Frontera, San Diego, CA 92127-1806, USA, walker@lh-systems.com

KEYWORDS: digital sensor, digital camera, digital photogrammetry, digital photogrammetric workstation, multispectral imagery, digital imagery.

ABSTRACT

Digital imagery from satellites or multispectral and hyperspectral scanners is well accepted. Tremendous challenges are inherent in the development of a digital sensor to acquire imagery suitable for both high precision photogrammetric mapping and image processing for interpretative purposes. The performance of the film aerial camera is almost impossible to reach with current digital technology. Joint development work by LH Systems and Deutsches Zentrum für Luft- und Raumfahrt (German Aerospace Centre) has produced encouraging results using forward-, nadir- and backward-looking linear arrays on the focal plane to provide panchromatic imagery and geometric information, supplemented by further arrays for multispectral data.

The geometric characteristics of line scanner imagery necessitate line by line rectification for aircraft tilts and shifts. Satisfactory execution of this process depends on supplementary data from high performance, on-board GPS and inertial measurement systems. Similarly, high demands are placed on other sub-systems, such as the camera mount, lens, electronics and storage technology. The software to process imagery from the sensor must meet several particular requirements arising from the three-line principle. In addition to rectification for aircraft tilts and shifts, rectification for terrain characteristics is also required in order to generate colour and false colour composite images, since the various multispectral arrays are in different places on the focal plane. The special geometry also impacts triangulation. Thereafter, the imagery can be processed using existing software packages from both photogrammetry and remote sensing.

The concept has been demonstrated in several successful test flights. The production model is scheduled for market introduction in mid-2000. The imagery from the new sensor will fulfil many market requirements between the highest resolution film imagery (<0.1 m) and high resolution space imagery (1-10 m). The sensor's unique blend of multispectral information with high quality geometric information will give rise to numerous new applications.

1. INTRODUCTION

LH Systems' announcement at the end of 1998 that an engineering model of their forthcoming airborne digital sensor had been flown successfully implies that a genuine alternative to the familiar aerial film camera is imminent.

Except for producing stereoscopes, LH Systems and its predecessor Leica were never active in image interpretation. Yet this new sensor will have multispectral lines on the focal plane: it will be capable of generating precise, geometric information about the surface of the earth, but will also produce data amenable to proven remote sensing techniques. It will further soften the demarcation between photogrammetry and remote sensing and accelerate the decline of the photo laboratory, as digital image data can be transferred from the aircraft directly to the workstation.

The debate about airborne versus spaceborne imagery continues. The highest resolution applications, with ground pixel sizes in the one centimetre to one decimetre level, are likely to remain the province of the film camera. Yet there is a huge, pent up demand for top quality, multispectral information in the gap between this and the one metre and coarser resolutions offered by the satellite operators. Both spaceborne and airborne

sensors have their advantages and the most likely scenario for the future will be an increased emphasis on data fusion as users select the sensors most likely to provide their information in each case and rely on their workstation software to use all the data together. The two types of data will be complementary rather than competitive.

2. AIRBORNE DIGITAL SENSORS: REQUIREMENTS

To have any chance of an impact in a market place spoilt for decades by high performance film cameras, an airborne digital sensor must provide:

- large field of view and swath width
- high resolution and accuracy, both geometric and radiometric
- linear sensor characteristics
- multispectral imagery
- stereo.

The first requirement, however, seems to rule out area CCD arrays, because readily available models in mid 1999 are 4Kx4K pixels or less, whereas a linear array of 12,000 pixels is readily available, requiring only one third as many flight lines. Considerable research work has been done in Germany since the 1970s, which has demonstrated the suitability of three panchromatic lines on the focal plane, with additional multispectral lines near the nadir. This obviates the need for multiple area arrays to provide a wide field of view and a multispectral capability (Figure 1). The left-hand diagram suggest how the focal plane could be populated using the three line principle: three panchromatic lines give the geometry and stereo, whilst additional lines, their sensitivity controlled by filters, give the multispectral information. In the right hand diagram, multiple area array CCDs and lenses are required to provide both the same ground pixel size and multispectral range as the three-line approach.

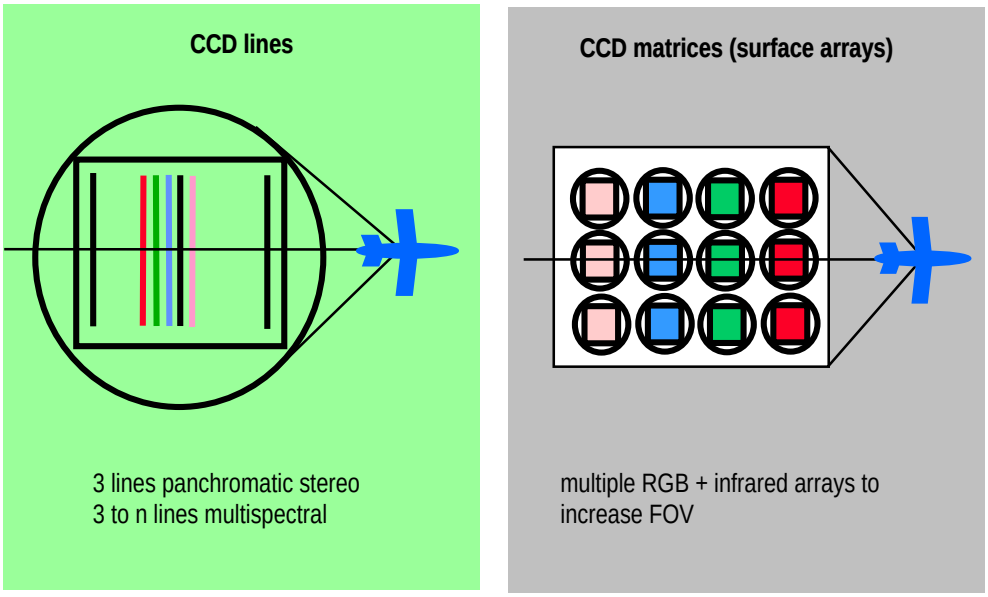

Fig. 1. The alternatives: linear and area CCD arrays.

3. THREE-LINE SCANNER APPROACH

The three-line concept results in views forward from the aircraft, vertically down and looking backwards (Figure 2). The imagery from each scan line is assembled into strips (Figure 3). The characteristics of relief displacement in the line perspective geometry of the strip approach *vis a vis* the conventional central perspective geometry are indicated in Figure 4, showing the line perspective geometry of the three-line imagery on the left and the familiar central perspective geometry of the film photograph on the right. The angles between the incoming information to the three lines are, of course, fixed. With three lines there are three possible pairings for stereoscopic analysis – strips 1 and 2, 2 and 3, and 1 and 3. With film cameras, the parallactic angle is a function of principal distance and airbase. Moreover, every object appears on all three strips, whereas on film imagery only 60% of the area of any one photograph is in a triple overlap.

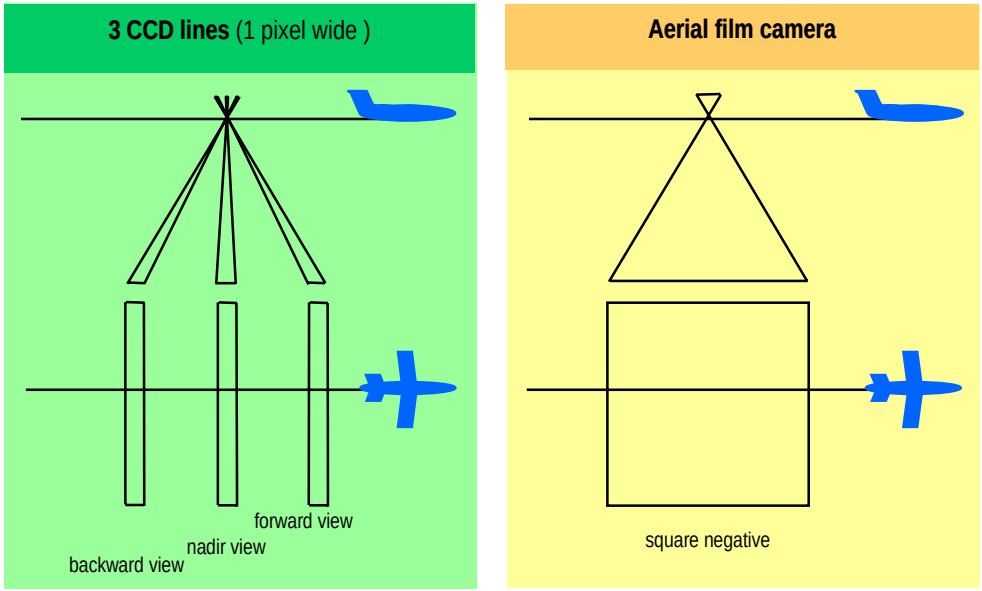

Fig. 2. Basic geometric characteristics of three-line digital sensor and film camera.

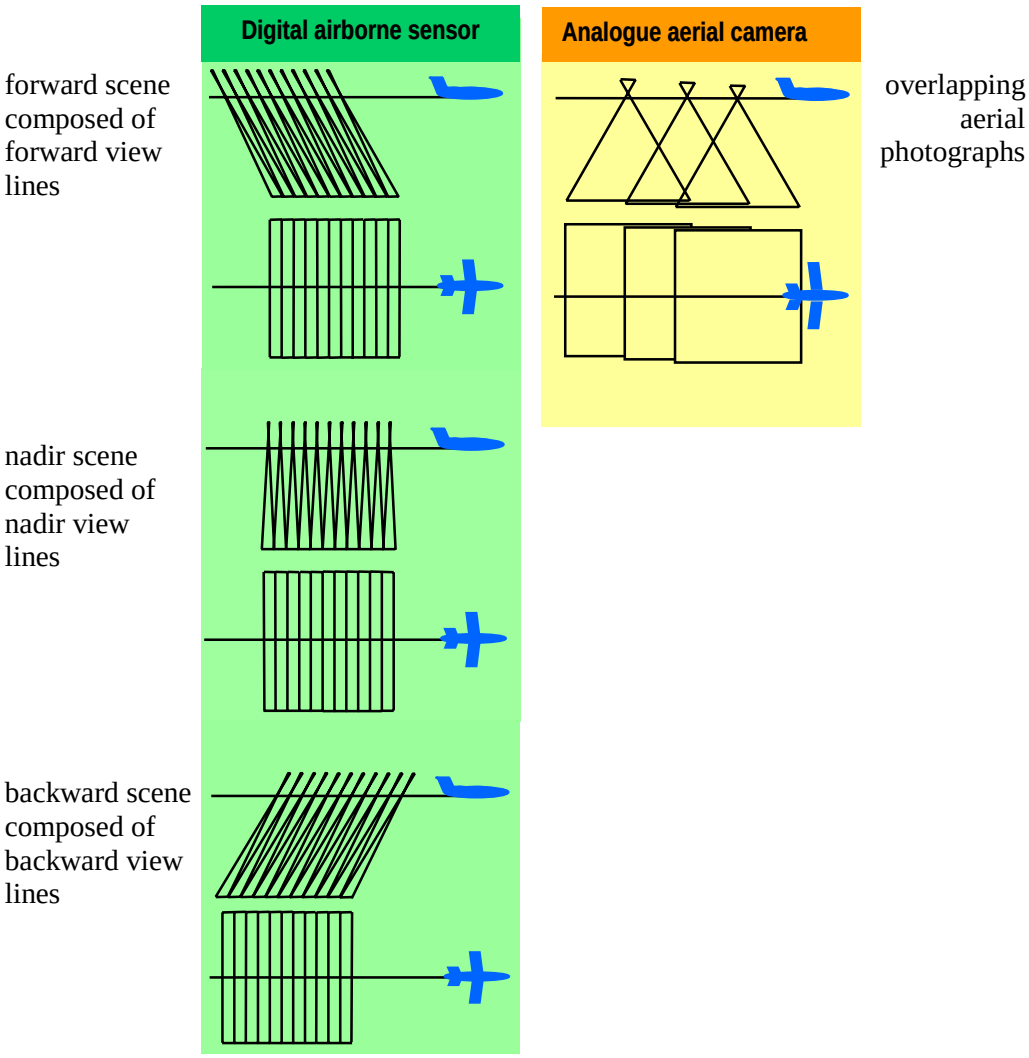

Fig. 3. Comparison of the acquisition of scenes by three-line digital sensor and film camera.

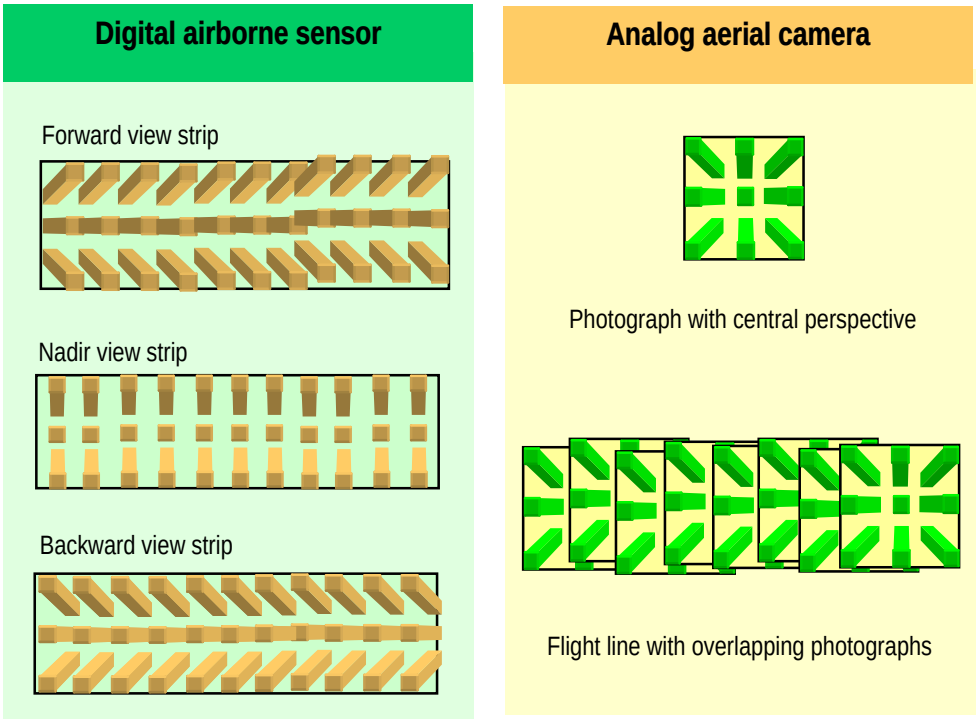

Fig. 4. Effect of terrain relief on the imagery

4. RADIOMETRIC CONSIDERATIONS

The best possible signal to noise ration (SNR) is a precondition for signal processing, digitising, data compression and data transfer with little interference. The signal to noise ratio of the elements of a CCD are given by:

$$SNR = \frac{n_s}{\sqrt{\sigma_s^2 + \sigma_{rms}^2 + \sigma_{fp}^2}} \qquad (1)$$

where n_s: signal electron count

σ_s^2: variance of signal electron count

σ_{rms}^2: variance of the time dependant noise

σ_{fp}^2: variance of local sensitivity differences (fixed pattern noise).

The signal electron count is directly proportional to the number of arriving photons (within a defined narrow wavelength interval). The noise of the signal electrons therefore is subject to the Poisson statistics of photon noise:

$$\sigma_s = \sqrt{n_s} \qquad (2)$$

The time dependent noise of the CCD and of the analogue channel (rms noise) contains:

- temporary dark signal noise (Poisson statistic)
- reset-noise and on-chip-amplifier noise ("kTC-noise")
- transfer noise
- other electronic noise (1/f - noise, thermal noise).

For estimation purposes the following calculations are based on a noise electron count of $\sigma_{rms} = 235e^-$.

The fixed pattern noise has two sources

- photo response non-uniformity (PRNU) of the CCD elements
- shading of the light intensity in the focal plane of a wide-angle optics.

Observing the behaviour of only one CCD element by ignoring the PRNU (photo response non-uniformity), e.g. the fixed pattern noise, we find the conditions shown in Figure 5, if we take into account a saturation electron count of >500,000. The SNR amounts to 8 or 9 bits (SNR = 250 ... 670) for an electron count >100,000.

If we now look at the real conditions in the focal plane of a wide-angle lens, we obtain the diagram of the signals at the outlet of a CCD line, as shown in Figure 6: flat field illumination creates in the focal plane of wide-angle optics a CCD signal including the effects of shading due to optics and PRNU.

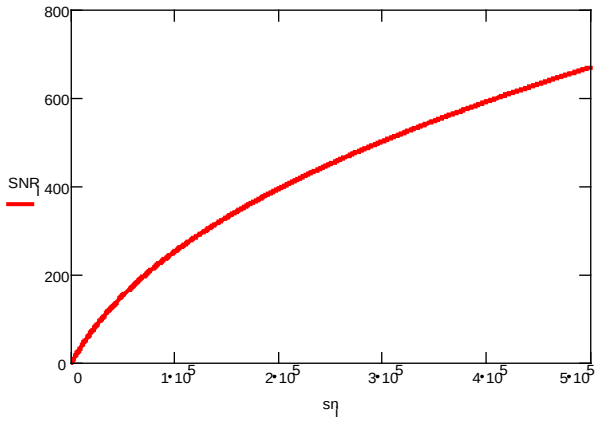

Fig. 5. SNR of a CCD-element at a saturation load of 500,000 electrons and rms-noise of 235 electrons.

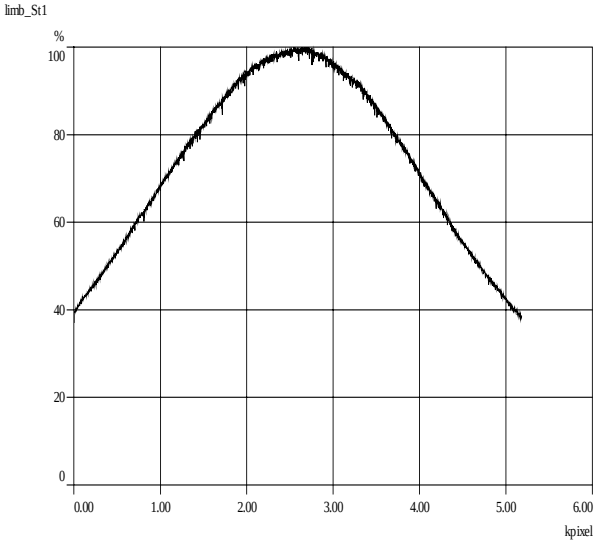

Fig. 6. Effect of flat field illumination in the focal plane.

One can clearly see the effect of the shading of the lens (at the edges the light intensity falls off to about 40%) and of the influence of the PRNU. The differences of sensitivity of CCDs are usually indicated in the datasheets as PRNU values in percent of the values of the videocurrent for the range far below saturation (mostly at 50% of U_{sat}). We will adhere to this definition here as well. Thus in the linear range of the CCD the fixed pattern noise of the pixel sensitivity can be expressed directly as a signal dependent noise, which is converted into a time dependent noise during transfer of the charge.

$$\sigma_{fp} = \frac{PRNU}{100\%} \cdot n_s = \frac{PRNU}{100\%} \cdot \sigma_s^2 \qquad (3)$$

Depending on the PRNU of the CCD the signal to noise ratio results as:

$$SNR = \frac{\sigma_s}{\sqrt{1 + \left[\frac{PRNU}{100\%} \cdot \sigma_s\right]^2 + \left[\frac{\sigma_{rms}}{\sigma_s}\right]^2}} \qquad (4)$$

Figure 7 shows the highest attainable SNR at full exploitation close to saturation (400,000 to 500,000 signal electrons) in relation to PRNU, based on the aforementioned parameters. Up to a PRNU value of 0.02% the SNR is determined exclusively by the photon noise of the signal, the rms noise of the CCD and the noise of the analogue channel. At 0.1% the PRNU influence becomes dominant. In the engineering model of LH Systems' new airborne digital sensor, described in sections 6 and 7 below, the PRNU correction is done pixel-wise.

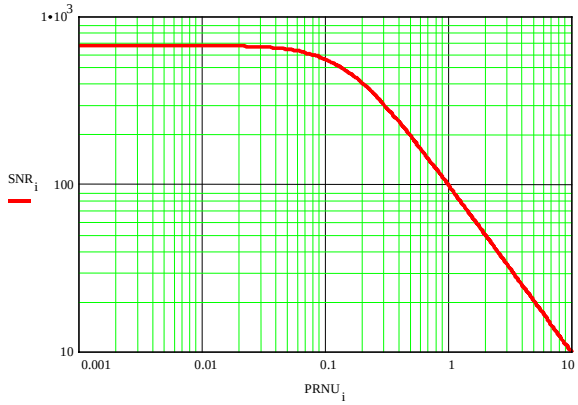

Fig. 7. SNR in relation to PRNU assuming a thermal and electronic noise of S_{el} = 235 rms-electrons and a signal electron counts of 500 000 e^-.

Normally light fall-off of the lens system (approximately 30%) is corrected simultaneously with the PRNU correction. For the estimation or the PRNU correction, this fall-off has not been taken into account because it does not contribute directly to an increase of the SNR. It only contributes indirectly through the adaptation of the signal to the analogue channel. The correction of light fall-off of the lens does not restrict the SNR significantly.

The efficiency of the correction can be seen in Figure 8, which shows imagery of the Reichstag, Berlin, taken with the engineering model of the LH Systems airborne digital sensor on 23 April 1999. The flying height was 3 km and the ground sample distance is 0.25 m. In the radiometrically zoomed-out image parts no noise can be seen.

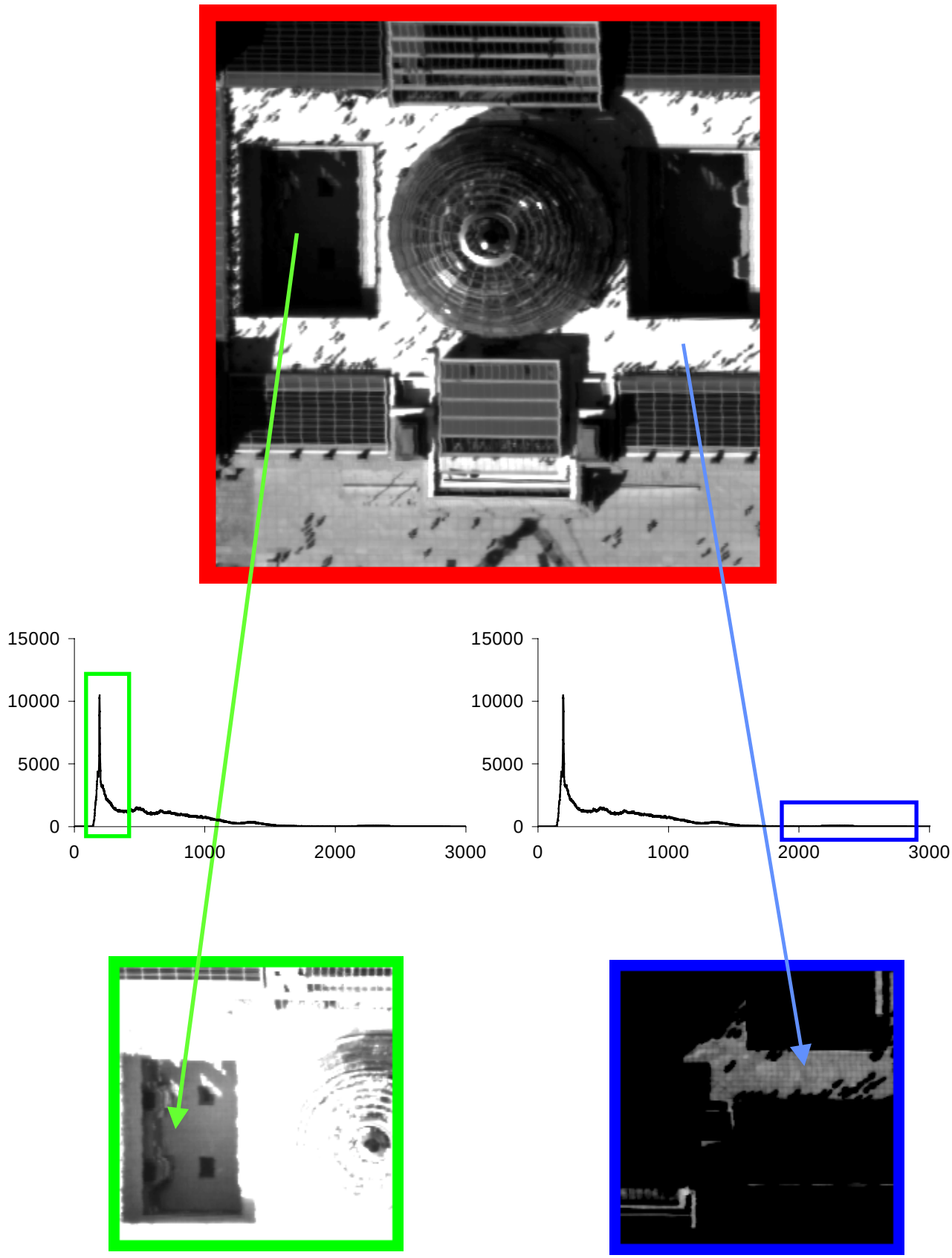

Fig. 8. Imagery of Berlin, taken with the engineering model of the LH Systems airborne digital sensor.

5. MTF CONSIDERATIONS

The geometrical resolution of the camera system essentially depends on the MTF of the system optics/CCD pixel. It describes the damping of the incoming radiation as a function of the spatial frequency. This may serve as a basis to define a contrast function.
Considering only this optics/CCD-pixel system, the MTF_{SYS} is calculated by multiplying the MTFs of the system constituents MTF_{OPTICS} and MTF_{PIXEL}

$$\mathbf{MTF}_{SYS} = \mathbf{MTF}_{OPTICS} * \mathbf{MTF}_{PIXEL} \qquad (5)$$

The MTF_{PIXEL} of the CCD pixel is:

$$\mathrm{MTF}_{PIXEL} = \frac{\sin(\pi \cdot k \cdot x)}{(\pi \cdot k \cdot x)} \qquad (6)$$

with k being the spatial frequency measurement in mm^{-1} and Δ being the pixel distance, here 6.5 µm.
The function MTF_{PIXEL} is shown in Figure 9.

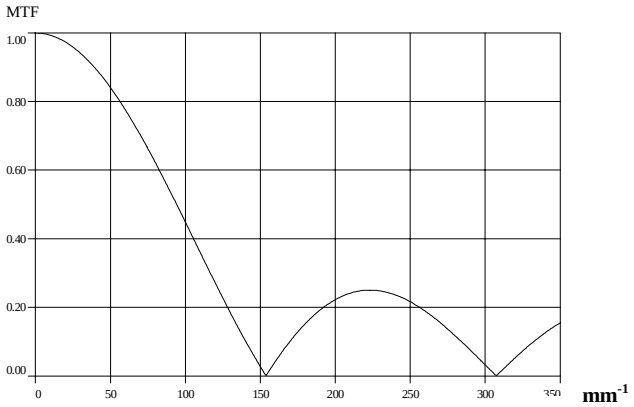

Fig. 9. MTF of CCD pixel, distance of pixel centers 6.5 µm.

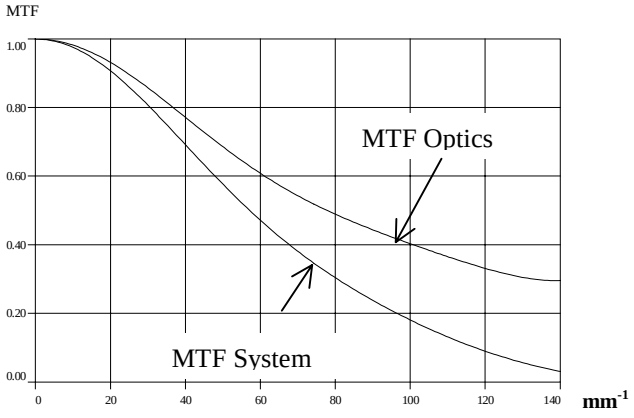

Fig. 10. MTF_{OPTICS} of MTF_{SYS} of the engineering model at the optical axis.
This Figure shows the MTF_{OPTICS} of the EM optics measured in the optical axis of the calibration laboratory of the DLR Institute for Space Sensor Technology in Berlin, Adlershof. The second curve in Figure 10 is the resulting MTF_{SYS} for the nadir looking pixel.
To allow for comparison with the MTF of the pixel given in Figure 9, a wider range of MTF_{SYS} is shown in Figure 11.

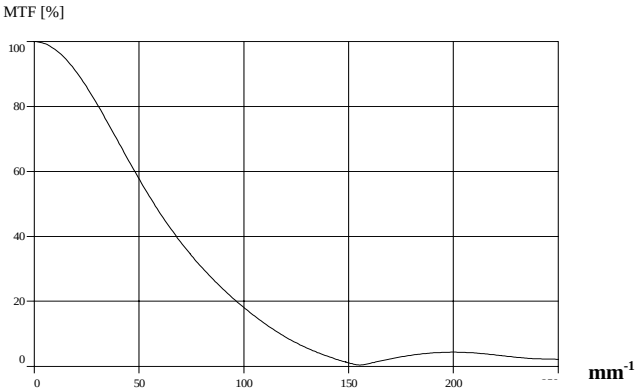

Fig. 11. MTF of a pixel near the optical axis of the engineering model

With a MTF_{SYS} of $\approx 30\%$ at the Nyquist frequency:

$$k_{NY} = \frac{1}{2\Delta} \qquad (7)$$

given for Δ = 6.5 µm, a number of k_{NY} = 77 Lp/mm (Linepairs per mm), the contrast potential and therefore the imaging quality of the EM is pretty good. This holds also for the non-nadir areas of the focal plane used by the nadir and stereo looking CCD lines, since the MTFSYS does not deviate dramatically form the shown curve. Figure 12 gives a measured curve for the centre of the stereo forward line (17°) in comparison with the centre of the nadir line.

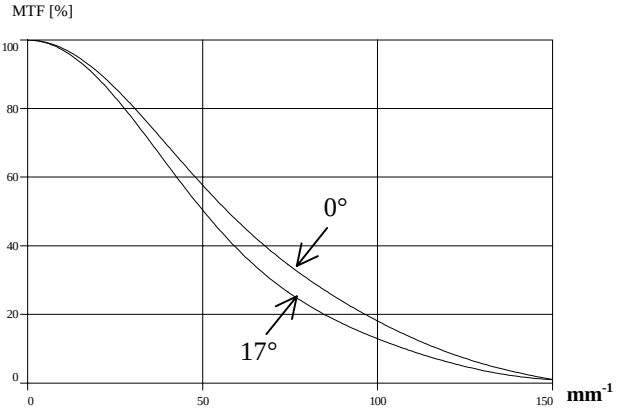

Fig. 12. MTF of centre of nadir line (0°) and centre of forward stereo line (+17°)

6. IMAGE PROCESSING

The raw imagery looks bizarre, because aircraft tilts and terrain relief cause the linear arrays to image widely varying strips of terrain, is well known. Figure 9 shows imagery acquired by the new sensor over Berlin. The flight direction was from left to right. The top image is raw. The bottom image has been rectified and looks similar to a conventional aerial photograph. Note the correspondence between the edges of the rectified image and the roll of the aircraft. Tilts have been compensated by adjusting each individual scan line for the attitude of the aircraft, using data from the airborne GPS and INS units carried on every fight. An initial rectification using these data is essential even to view the imagery. Thereafter, operations such as triangulation, DTM measurement, orthophotos and feature extraction continue in the usual way. Automated processes, such as point measurement for triangulation and DTM extraction, can be based on triplet matching using the three strips.

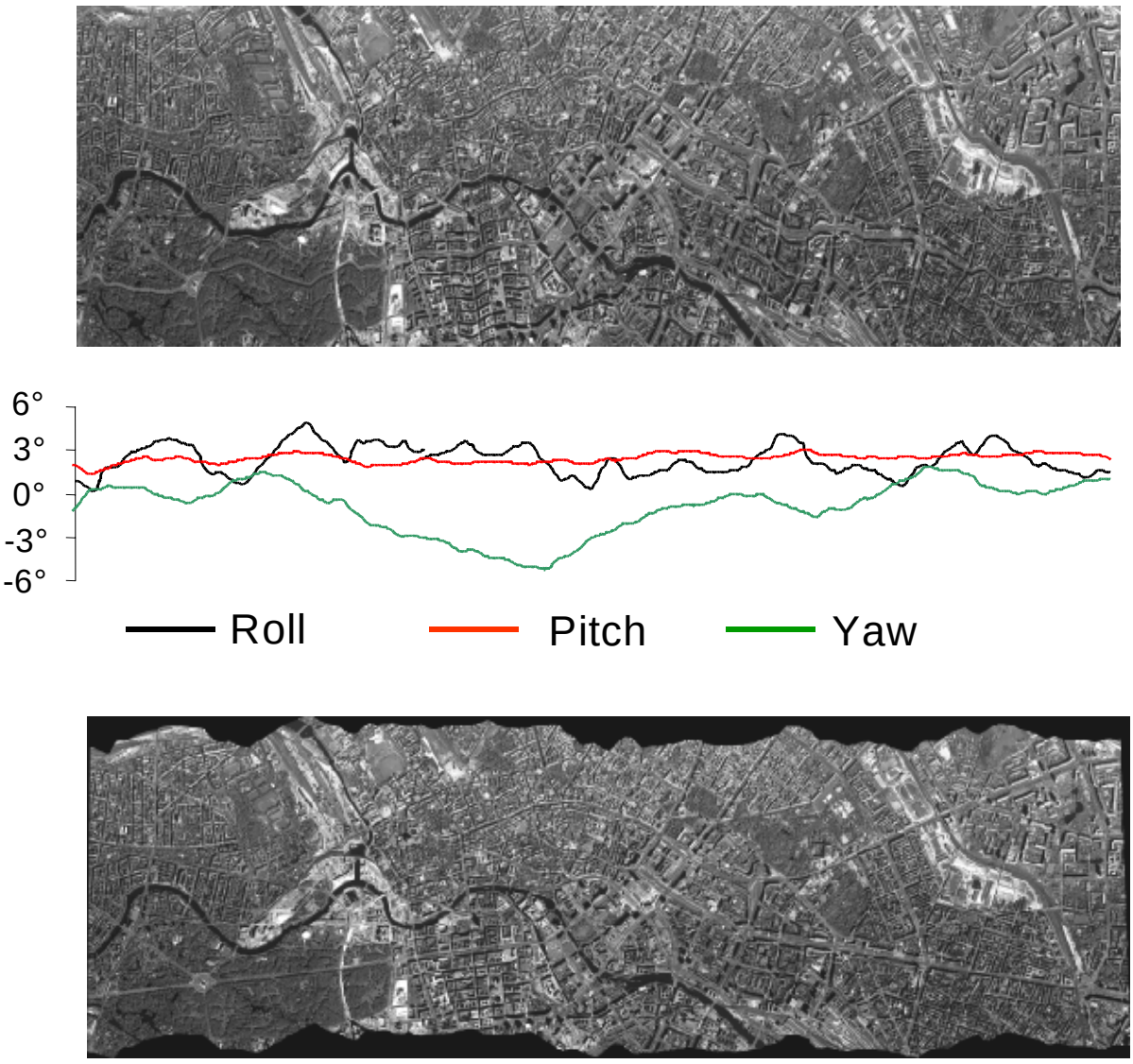

Fig. 13. Imagery acquired by the new sensor over Berlin.

Owing to their positions on the focal plane, combined with the aircraft and terrain variations, the colour lines image slightly different parts of the earth's surface. Thus full rectification is required, i.e. orthophotos are produced, before the colour bands can be properly registered and transformed into colour composite images suitable for analysis by off-the-shelf remote sensing packages.

7. ENGINEERING MODEL AND TECHNICAL CO-OPERATION

The complexity, cost and difficulty of developing and manufacturing a novel airborne digital sensor ruled out "going it alone". In early 1997, shortly before LH Systems was formed, Leica Geosystems reached a technology agreement with Deutsches Zentrum für Luft- und Raumfahrt (DLR), the German Aerospace Centre in Berlin. This provided for long term co-operation, with joint development by both parties and assembly by Leica Geosystems. DLR's experience in this area is unparalleled. Amongst a host of intricate and impressive achievements in both airborne and spaceborne technology, it made historic progress with sensors based on the three-line approach, for example the WAOSS (Wide Angle Optical Stereo Sensor, built for the unfortunate Mars-96 mission) (Sandau and Bärwald, 1994), WAAC (Wide Angle Airborne Camera) (Sandau and Eckhardt, 1996) and HRSC (High Resolution Stereo Camera) (Albertz *et al.*, 1996). The technical and performance data of WAOSS and WAAC are summarised in Table 1. DLR's expertise complemented well Leica Geosystems' abilities in optics, mechanics and electronics, together with its deep appreciation of customers' requirements acquired through decades of producing aerial film cameras. It was natural that the agreement between the parties be transferred to LH Systems quite soon after its formation.

8. PRACTICAL CONCLUSIONS

The features of the film and digital approaches are compared in Table 2. LH Systems has chosen the three-line scanner approach for the reasons given above. The engineering model has flown (Figure 10, Table 3) and work is proceeding towards the production model, which will have at least 20,000 pixels in each line, faster integration times and multispectral bands.

This is on schedule for launch at the ISPRS Congress in Amsterdam. The formidable technical challenges can be met. Perhaps the real hurdle will by then have moved: photogrammetrists will learn to work with imagery that is strikingly different in appearance from the film case and is processed using unfamiliar sensor models. They will be able to share data with the remote sensing community and for the first time create deliverables with both the depth of information accruing from image understanding of multispectral images and the geometric fidelity of photogrammetry.

	WAOSS	**WAAC**
Focal length, f	21.7 mm	21.7 mm
FOV (across track)	$\leq 80^{o}$	$\leq 80^{o}$
Optics	Spitmo-Russar-96	Spitmo-Russar-96
CCD lines	3	3
Spacing of CCDs	10.1 mm	10.1 mm
Convergence angle	25^{o}	25^{o}
IFOV (quadratic)	3.23×10^{-4} rad	3.23×10^{-4} rad
Elements per CCD-line	5184	5184
Elements spacing	7 µm	7 µm
platform height	250 km	5 km
Swath width (nadir)	420 km	8.4 km
Minimum ground resolution - in line direction - in trajectory direction	 80 m 80 m	 1.6 m 1.6 m
Dynamic range	11 bit	11 bit
Radiometric resolution	8 bit	8 bit
Spectral channel - nadir - forward, backward	 470...670 nm 580...770 nm	 580...770 nm 470...670 nm
Data compression factor	2...20	2...20
Data compression method	DCT- JPEG	DCT- JPEG
Output science data rate	100...500KBit / s	100KBit / s...24MBit / s
Physical dimensions	L:373 x B:190 x H:218 mm	L:285 x B:190 x H:202 mm
Mass	8 kg	4.4 kg
Power	18 W	15W

Table 1. Technical and performance data of WAOSS and WAAC.

In the standard version of the new airborne digital sensor the multispectral images will be derived from the data captured with four CCD sensors equipped with appropriate filters in the RGB and NIR bands. These data will be used to produce true-colour and false-colour composites based on the orthophotos derived from the panchromatic three-line CCD sensors.

Characteristic	Aerial film camera	Airborne digital sensor
Flying time	20% less	-
Photo lab	Yes	No
12-bit in-flight sensing	No	Yes
8/10-bit scanning	Yes	Unnecessary
Data volume	20-50% less	
Pre-processing	No	Yes
GPS	Yes (optional)	Yes
INS	Unusual	Yes
Projection centres	Interpolated (few)	Interpolated (many)
Ground control points	Yes, but hardly any with GPS	Yes, but hardly any with GPS
Tie point matching	Few – between images	Many

Table 2. Features of aerial film camera and airborne digital sensor

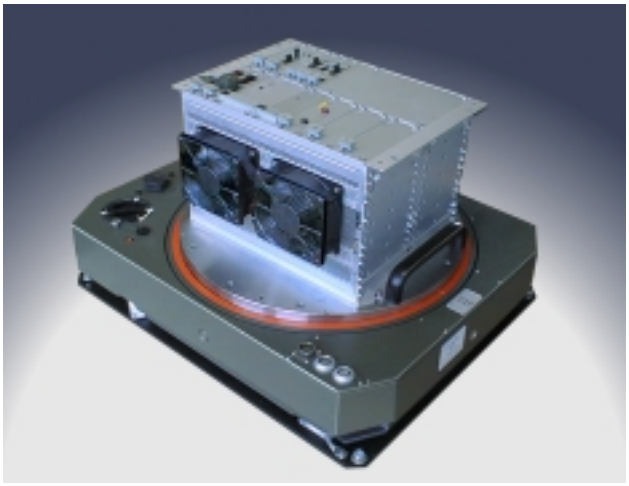

Fig. 10. The engineering model of LH Systems' airborne digital sensor, which was successfully flown in late 1998.

It is LH Systems intention to make the data format of these images accessible to all third party remote sensing software packages used for image enhancement and image analysis. LH Systems own SOCET SET software will provide basic image enhancement functions.

General	
Principle	3 line CCD stereo sensor
Pixels per CCD Line	12,000
Pixel size	6.5 µm
Dynamic range	12 bit (raw data mode)
Radiometric resolution	8 bit
Normalisation mode	8 bit linear or non-linear
FOV (across track)	52°
Focal length	80 mm
Swath at 10,000' flying height (3,100 m)	3,000m (1.9 miles) and 25 cm ground pixel size
Stereo angles	17°, 25°, 42°
Recording interval per line	1.2 ms
Filter range (at λ50)	Panchromatic, 465nm – 680nm

Power	
Input voltage	28 VDC or 220 VAC/50 Hz
Consumption / average (peak)	Engineering model: 600 W (1000 W)
	Mass memory system: 600 W (600 W)
	ASCOT: 80 W (180 W)

Table 3. Specifications of the engineering model.

ACHNOWLEDGMENTS

The authors thank DLR for its contributions to the development of the engineering model and the test flights. We owe special thanks to Dr. Reinhard Schuster who provided the engineering model calibration results used in this paper.

REFERENCES

Albertz, J., Ebner, H. and Neukum, G., 1996. The HRSC/WAOSS camera experiment on the MARS96 mission – A photogrammetric and cartographic view of the project. 18th ISPRS Congress, Vienna, July 9-14.

Sandau, R. and Bärwald, W., 1994. A three-line wide-angle CCD stereo camera for Mars-94 mission. In: International Archives of Photogrammetry and Remote Sensing, Vol. 30, Part B1, pp. 82-86.

Sandau, R. and Eckardt, A., 1996. The stereo camera family WAOSS/WAAC for spaceborne/airborne applications. In: International Archives of Photogrammetry and Remote Sensing, Vol. 31, Part B1, pp. 170-175.